

# Currents Induced in an Anatomically Based Model of a Human for Exposure to Vertically Polarized Electromagnetic Pulses

Jin-Yuan Chen, *Member, IEEE*, and Om P. Gandhi, *Fellow, IEEE*

**Abstract**—The finite-difference time-domain (FDTD) technique is used to calculate the internal fields and the induced current densities in anatomically based models of a human using 5628 or 45 024 cubical cells of dimensions 2.62 and 1.31 cm, respectively. A layer of dielectric constant  $\epsilon_r = 4.2$  and thickness 2.62 cm is assumed under the feet to simulate a human wearing rubber-soled shoes. The total induced currents for the various sections of the body and the specific absorptions for several organs are given for two representative electromagnetic pulses. The calculated results for the induced currents are in excellent agreement with the data measured for a human subject. The FDTD method is ideally suited for exact representation of the pulse shapes and offers numerical efficiency to allow detailed modeling of the human body and the various organs.

## I. INTRODUCTION

HIGH-INTENSITY electric and magnetic fields associated with an electromagnetic pulse (EMP) have resulted in public concern regarding the potential health effects. Electric fields as high as 60–100 kV/m and magnetic fields that are approximately 1/377 times lower have been measured close to EMP generators. The fields are, of course, considerably lower at larger distances from these generators. The EMP's are marked by rise times of the order of 10–30 ns with pulse durations of the order of 100–300 ns.

Approximating the human body by three cylinders of uniform conductivity, one vertical and two horizontal to represent shoulders, Grønhaug has calculated currents induced for exposure to an EMP [1]. Guy, on the other hand, has used a model consisting of 12 cylindrical sections, each representing approximately a 15 cm height of the human body [2]. These sections are loaded with parallel *RC* circuits representing the measured impedance for a human subject for the corresponding sections of the body. Approximating the incident EMP by an expression  $E(t) = K[\bar{e}^{\alpha t} - \bar{e}^{\beta t}]$ , currents for various frequency components (75 frequencies covering the range 100 Hz to 300 MHz) are calculated using the NEC 2D code detailed in Burke and Poggio [3]. The induced current in the time domain for the minimum area section representing the feet and ankles is then obtained from the Fourier transform of the currents calculated for the various frequencies.

Manuscript received February 13, 1990; revised July 24, 1990. This work was supported by the USAF School of Aerospace Medicine, Brooks AFB, Texas.

The authors are with the Department of Electrical Engineering, University of Utah, Salt Lake City, UT 84112.

IEEE Log Number 9040564.

Since these models are fairly gross approximations, we have used the previously described anatomically based model of a human to calculate currents induced in the human body for exposure to a few representative EMP's. The finite-difference time-domain (FDTD) technique [4]–[10] was used to calculate the internal fields ( $E$ ) and the current densities ( $J$ ) for each of the cubical cells of dimensions 2.62 cm (5628 cells) or 1.31 cm (45 024 cells) that are used to describe the human body. As previously described [4]–[6], the volume-averaged dielectric properties and mass densities were obtained from the contents of these subvolumes in terms of the 16 tissues and air. The information on the tissue contents was obtained with a resolution of 1/4 in. from the anatomical diagrams [11]. The models were assumed with a layer of dielectric constant  $\epsilon_r = 4.2$  of thickness 2.62 cm under the feet to simulate a human wearing rubber-soled shoes. This assumed thickness corresponds to the width of one or two cells for the two models, respectively.

Being a time-domain technique, the FDTD method is ideally suited for calculations involving EMP's. Exact pulse shapes can be modeled by using small time increments. This method does, however, require that the dielectric properties of the body be nondispersive, i.e., independent of frequency in the band representing the frequency content of the EMP. This requirement, unfortunately, is not met for the human tissues which are known to be dispersive. A rigorous approach to this problem using the FDTD method would therefore require the solution of Maxwell's equations coupled to the polarization equations in the time domain for the various tissues. Since the scope of the present project did not call for a full-blown effort in this regard, we have used an approximate model that uses the dielectric properties at 40 MHz. This is somewhat justified since the predominant components of the induced current are at frequencies close to 40–50 MHz, which is near the resonant frequency of an adult human standing on a ground plane [12].

## II. FDTD METHOD

The FDTD method was first proposed by Yee [7] and later developed by Umashankar and Taflove [8], Holland [9], and Kunz and Lee [10]. As mentioned above, we have recently used it for bioelectromagnetic problems [4]–[6], [13], [14]. In this method, described in detail in [8]–[10], [13], and [14], the coupled Maxwell equations in the differential form are solved for various points of the scatterer as well as its surroundings in a time-stepped manner until converged solutions are ob-

tained. To ensure stability, the time step  $\delta t$  is given by  $\delta/2v$ , where  $\delta$  is the cell size and  $v$  the maximum velocity of the electromagnetic (EM) wave encountered anywhere in the modeled space, which includes the human model and the surroundings. For our application,  $v = c$ , which is the velocity of the EM waves in air. We have taken  $\delta t = \delta/2c$  to be 0.04367 and 0.02183 ns for the 2.62 cm and 1.31 cm cell size models, respectively. These time steps are quite small compared with the duration of the EMP and are therefore able to represent the exact pulse shape very accurately.

The entire modeled space is divided into cubical cells with the cell size  $\delta$ , which should be smaller than or equal to one tenth of the smallest wavelength of EM energy encountered anywhere in the modeled space. This would imply a cell size  $\delta \leq \lambda_e/10$ , where  $\lambda_e$  is the wavelength at the highest irradiation frequency in high-water-content tissue such as muscle. Referring to wavelengths  $\lambda_e$  within muscle and high-water-content tissues [15], the models with cell sizes of 2.62 and 1.31 cm are therefore capable of representing frequencies up to 110 and 260 MHz, respectively. These frequency limitations are not unduly restrictive for the EMP's that have been considered to date. Since the modeled space must be restricted in size because of the computer memory limitations, absorption boundary conditions are used at the boundaries to simulate radiation into free space.

A sectional view of the geometry of the modeled space is shown in Fig. 1. The modeled space (along  $xyz$  directions, respectively) is divided into  $38 \times 26 \times 78 = 77064$  cells for the 2.62 cm resolution (nominal 1 in.) model and  $76 \times 52 \times 156 = 616512$  cells for the 1.31 cm resolution (nominal 1/2 in.) model. Of these, a total of 5628 cells or 45024 cells are either totally or partially within the human body, respectively. To simulate plane-wave irradiation uniform in phase, incident fields (vertically polarized  $E$  fields and  $x$ -directed  $H$  fields) of prescribed time variation are defined over a source plane located at a distance  $3\delta$  to the left of the absorbing plane in front of the model. The external absorbing boundaries are placed at a distance of  $7\delta$  or more ( $14\delta$  or more for the 1.31 cm model) on all sides of the human model. To reduce the modeled space, it is desirable to bring the absorbing boundaries as close to the region of interest as possible while still adequately simulating the actual interaction in question. We have verified the adequacy of the above separations from the absorbing boundaries by modeling plane-wave irradiation of lossy homogeneous and layered spheres at 27 and 100 MHz. Results of the calculated  $E^2$  variations for 58 (13.1 cm) or larger separations from the absorbing boundaries on all sides were found to be in excellent agreement (within 5%) with the analytic Mie solutions for the spheres [16].

To simulate the shoe-wearing condition, a separation layer of rubber ( $\epsilon_r = 4.2$ ) that is 2.62 cm thick is assumed between the feet of the model and the ground plane. This value of the dielectric constant has been estimated by measuring the equivalent capacitance of an electrical safety shoe (size 11, Vibram Manufacturing Company) with a Hewlett Packard model 4815A vector impedance meter over the frequency range 0.5–60 MHz. Also,  $\epsilon_r = 4.2$  is close to the values given in reference handbooks for neoprene rubber.

The perfectly conducting ground plane underneath the rubber is modeled in one of two ways: 1) by cells of high conductivity,  $\sigma = 3.72 \times 10^7$  S/m, corresponding to that of aluminum, or 2) by assuming that the tangential fields  $E_x$

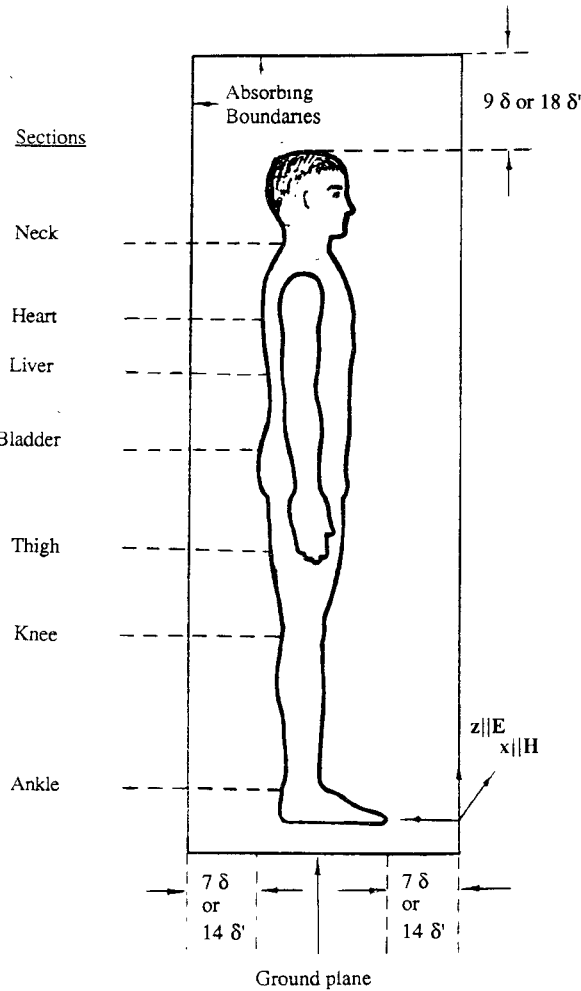


Fig. 1. Geometry of the modeled space for irradiation by EMP.  $\delta = 2.62$  cm for the 5628-cell coarser model and  $\delta' = 1.31$  cm for the higher resolution 45024-cell model of the human.

and  $E_y$  are always zero at the ground plane. Both procedures yield identical results for the fields and the currents calculated within the body.

For the present calculations, several steps have been taken to improve the efficiency of the FDTD code compared with the procedure described in the past [13], [14]. A major problem with this code is the large amount of memory storage that is needed. This is of the order of  $MN$ , where  $M$  is the number of parameters that need to be stored (for the algorithm used in the past [13], [14],  $M = 27$ ) and  $N$  is the number of cells into which the interaction region is divided ( $N = 77064$  for 2.62 cm resolution model and 616512 for 1.31 cm resolution model). In modifying the FDTD code, we have reduced the parameters ( $M$ ) that need to be stored. First, the tissue conductivities  $\sigma_x, \sigma_y, \sigma_z$  and permittivities  $\epsilon_x, \epsilon_y, \epsilon_z$  that were previously stored for all  $N$  cells at half-cell intervals have been replaced by single volume-averaged values of  $\sigma$  and  $\epsilon$  for each of the cells, resulting in a considerable reduction in the number of parameters that need to be stored. This step has also resulted in the intermediate property-dependent factors such as  $CA_x, CA_y, CA_z, CB_x, CB_y$ , and  $CB_z$  [14] being replaced by  $CA$  and  $CB$  for each of the

cells, defined as follows:

$$CA(i, j, k) = \left[ 1 - \frac{\sigma(i, j, k)\delta t}{2\epsilon(i, j, k)} \right] \left[ 1 + \frac{\sigma(i, j, k)\delta t}{2\epsilon(i, j, k)} \right]^{-1} \quad (1)$$

$$CB(i, j, k) = \frac{\epsilon_0}{4} \left[ \epsilon(i, j, k) + \frac{\sigma(i, j, k)\delta t}{2} \right]^{-1} \quad (2)$$

where  $(i, j, k)$  corresponds to values of these parameters at the center point of the cell at  $(i\delta, j\delta, k\delta)$ . Whereas  $CA_x$ ,  $CA_y$ ,  $CA_z$ ,  $CB_x$ ,  $CB_y$ , and  $CB_z$  were stored for each of the  $N$  cells in the past because of the different values of  $\sigma$  and  $\epsilon$  for the three directions, respectively, the new modified algorithm does not store  $CA$  and  $CB$  but rather calculates these parameters for each of the cells as needed with no detectable loss in efficiency of the code. The steps taken to date have reduced the memory-storage requirement by a factor of 2.7 ( $M$  reduced from 27 to 10) so that it is possible to solve the high-resolution 600 000 cell problem within the 64 Mbyte memory of the APOLO model 10000 workstation (the actual memory used was 26.6 Mbytes). These improvements have also reduced the computation time by roughly a factor of 2, e.g., for the 2.62 cm model from 8 min to 5 min using the CRAY XMP (available at the San Diego Supercomputer Center) while showing a negligible difference in the calculated results.

The calculated electric fields are used to obtain the currents for the various layers and the energy,  $W$ , absorbed by the model (or its parts) for the entire duration of the EMP. The following relationships are used:

$$I_k = \delta^2 \sum_{i,j} \left[ \sigma(i, j, k) E(i, j, k) + \epsilon_0 \epsilon(i, j, k) \frac{\partial E(i, j, k)}{\partial t} \right] \quad (3)$$

$$W = \delta^3 \delta t \sum_n \sum_{i,j,k} \sigma(i, j, k) |E(i, j, k)|^2 \quad (4)$$

where summation over  $i, j$  means summation for all cells in a given layer  $k$ , and summation over  $n$  means summation for all iterations in time for which  $E$  is nonzero.

### III. AN ANATOMICALLY BASED INHOMOGENEOUS MODEL OF THE HUMAN

As in [4] and [13], the inhomogeneous model of the human body is taken from the book *A Cross-Section Anatomy* by Eycleshymer and Schoemaker [11]. This book contains cross-sectional diagrams of the human body which were obtained by making cross-sectional cuts at spacings of about 1 in. in human cadavers. The process for creating the data base of the man model was as follows: a quarter-inch grid was taken for each single cross-sectional diagram and each cell on the grid was then assigned a number corresponding to one of the 16 tissue types (muscle, fat, bone, blood, intestine, cartilage, liver, kidney, pancreas, spleen, lung, heart, nerve, brain, skin, eye) or air. Thus the data associated with a particular layer consisted of three numbers for each square cell:  $x$  and  $y$  positions relative to some anatomical reference point in this layer, usually the center of the spinal cord; and an integer indicating which tissue that cell contained. Since the cross-sectional diagrams available in [11] are for somewhat variable separations, typically 2.3–2.7 cm, a new set of equispaced layers was defined at 1/4 in. intervals by interpo-

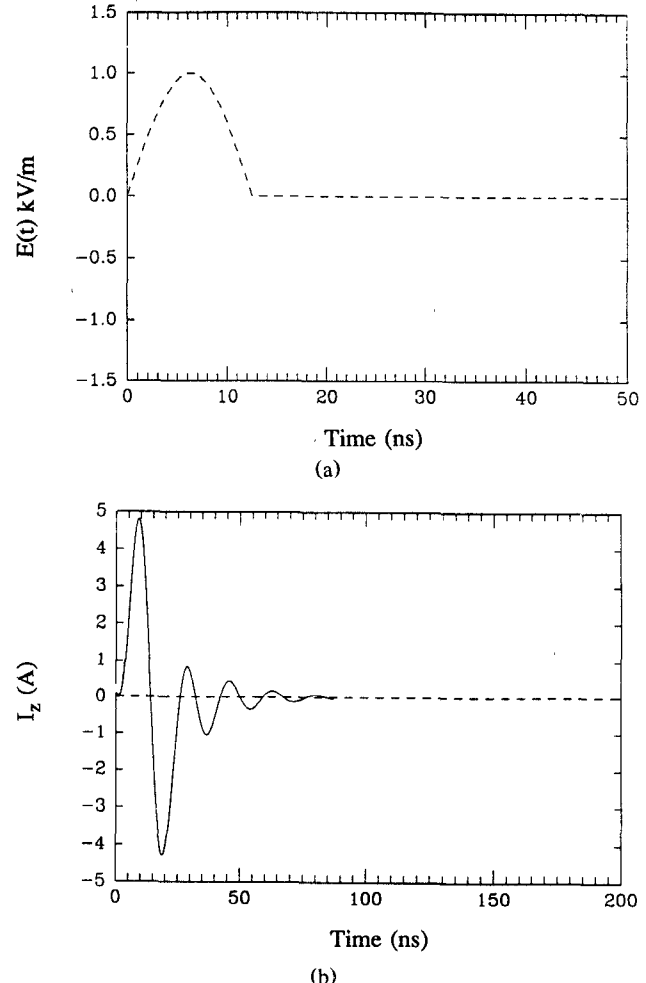


Fig. 2. The incident field and the current calculated for the section through the knees for a half-period sine wave pulse of duration 12.5 ns. Peak incident field = 1 kV/m. (a) The pulse wave form (note the considerably shorter time duration of the incident pulse compared with the duration for the current given in Fig. 2(b). (b) Current for the section through the knees.

lating the data onto these layers. Since the 1/4 in. cell size is too small for the memory space of present-day computers, the proportion of each tissue type was calculated next for somewhat larger cells, 1/2 in. or 1 in., combining the data for  $2 \times 2 \times 2 = 8$  or  $4 \times 4 \times 4 = 64$  cells of the smaller dimension, respectively. Without changes in the anatomy, this process allows some variability in the height and weight of the body. We have taken the final cell sizes of 1.31 or 2.62 cm (rather than 1/2 in. or 1 in. in the original model) to obtain the total height and body weight of 175.5 cm and 69.6 kg, respectively.

### IV. RESULTS

In this section, we give the calculated results for three representative EMP's, which are sketched in Figs. 2(a), 3(a), and 5, respectively. All of the incident  $E$  fields at the initial boundary plane (see Fig. 1) are assumed to be vertically polarized to obtain maximum coupling to the body. The EMP in Fig. 2(a) is an idealized sine wave with a duration of one half the time period at 40 MHz. This gives a time duration of 12.5 ns. A peak field of 1 kV/m is assumed for

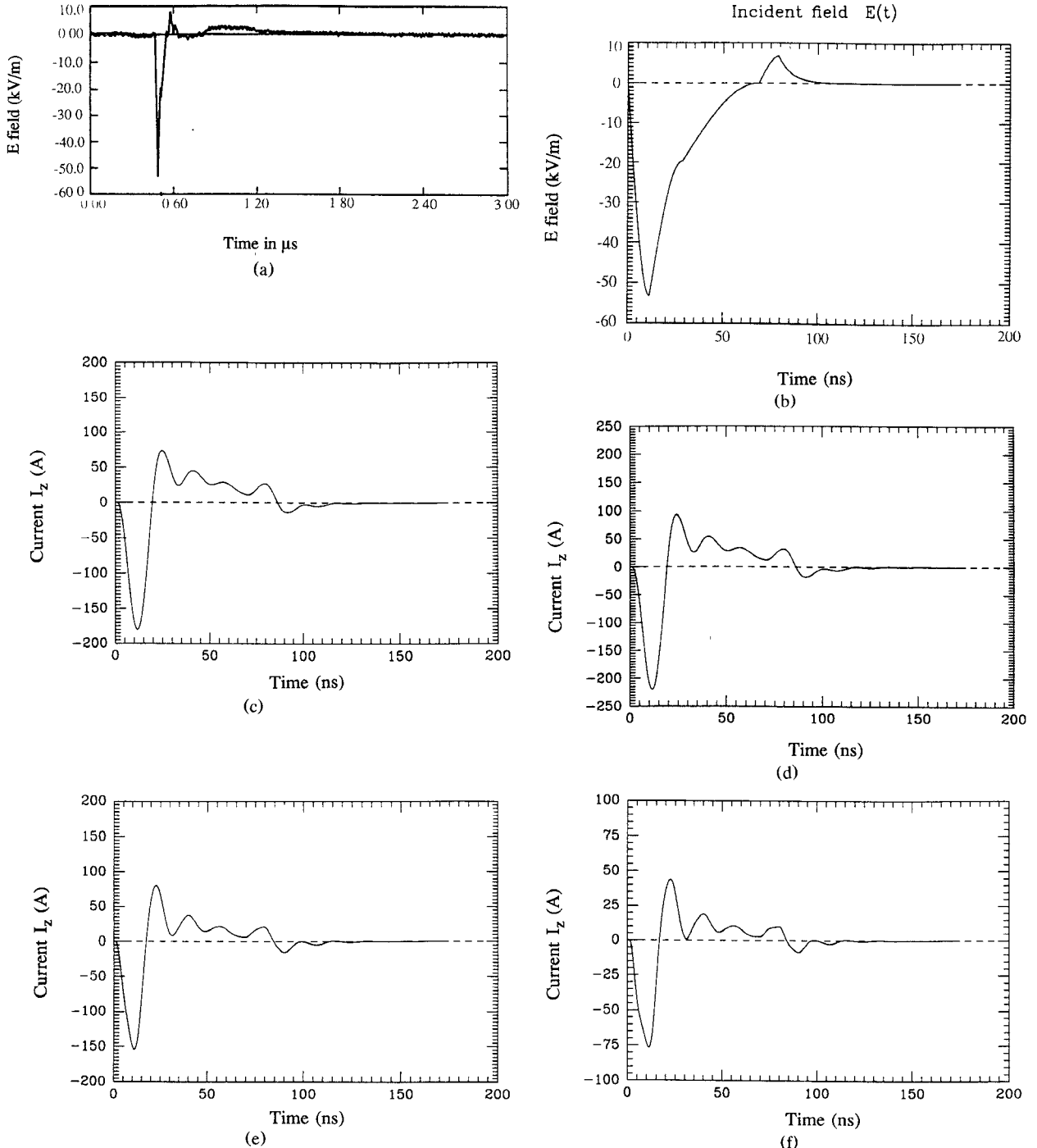


Fig. 3. Currents induced for a representative EMP. Peak incident field =  $-53,330$  V/m. (a) The measured pulse shape. (b) Simulated electric pulse (given by Eq. 5) plotted on an expanded scale. (c) Current for the section through the ankles. (d) Current for the section through the knees. (e) Current for the section through the heart. (f) Current for the section through the neck.

this pulse. Using (3), vertical, or  $z$ -directed, currents are calculated for each of the cells and summed up for a given layer to obtain the total current for that particular layer of the body. The time variation of current for the section through the two knees is shown in Fig. 2(b). Fairly similar ringing-type current variations were also obtained for the sections through the ankles, the heart, and the neck even though the peak magnitudes were somewhat different. For

the assumed incident peak field of 1 kV/m, peak currents of 3.9, 3.0, and 1.6 A were calculated for sections through the ankles, the heart, and the neck, respectively. For each of the sections it was interesting to note a ringing of the induced current with an approximate time period of 23.5 ns corresponding to a frequency of 42.5 MHz, which is close to the resonance frequency of a human standing on a ground plane [12].

TABLE I  
COMPARISON OF MEASURED AND CALCULATED VALUES  
(PEAK  $E \approx 55.4$  kV/m)

Section of Body	Peak Current Measured* A	Peak Current Calculated A
Both ankles	220	192
Both knees	244	235
Both thighs	284	—
Neck	100	81

Measured values are for a 5 ft, 6 in. female with shoes.

Time duration for half cycle of current is  $\sim 17$  ns both for measured and calculated currents.

\*Data courtesy of Wayne Hammer Naval Surface Warfare Center, White Oak, MD.

TABLE II  
SPECIFIC ABSORPTIONS (SA) IN MJ/kg FOR THE VARIOUS ORGANS  
AND THE WHOLE BODY FOR THE EMP'S OF FIGS. 3 AND 5

Organ	EMP of Fig. 3*	EMP of Fig. 5**
	SA mJ/kg	SA mJ/kg
Brain	0.026	0.016
Heart	0.05	0.029
Lung	0.053	0.029
Liver	0.068	0.034
Kidney	0.067	0.037
Ankle	8.55	4.37
Whole body	0.43	0.22

\* $E_{\text{peak}} = -53.5$  kV/m.

\*\* $E_{\text{peak}} = 41.5$  kV/m.

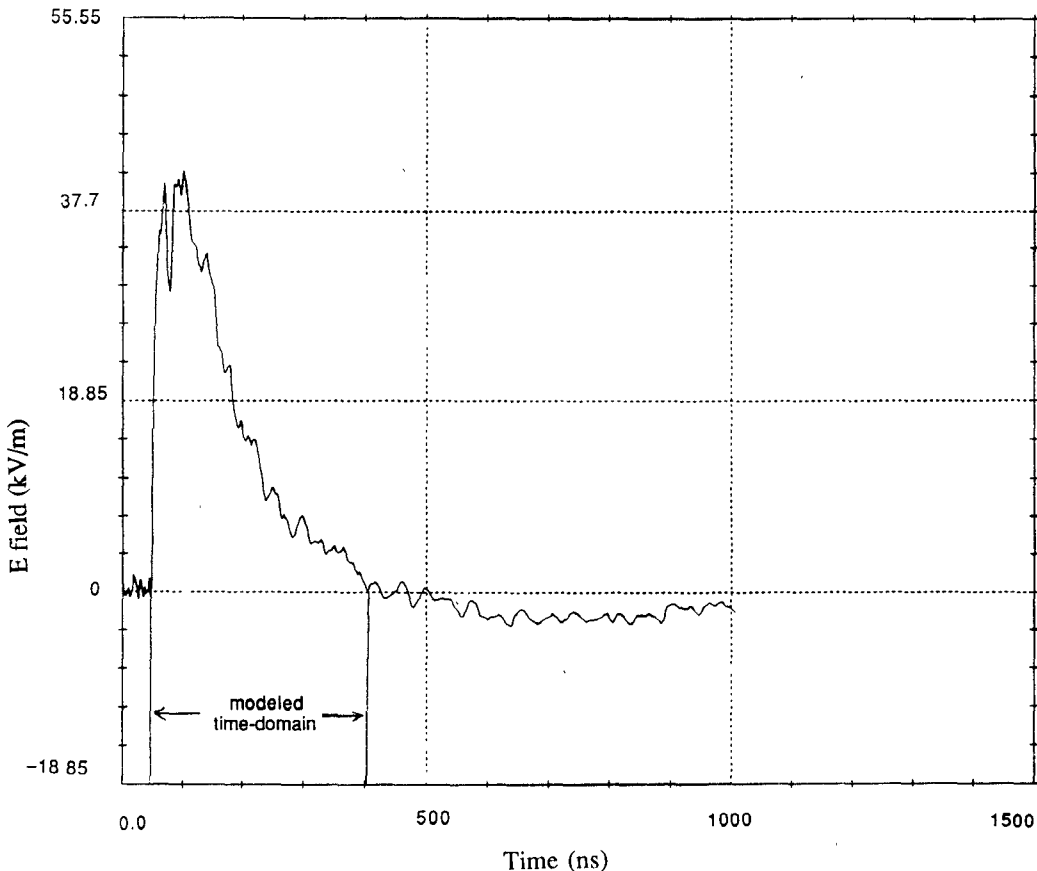


Fig. 4. The prescribed electromagnetic pulse. Peak incident field = 41.5 kV/m.

Next, a curve-fitting procedure was used to prescribe the time variation of the experimentally determined field shown in Fig. 3(a). The following closed-form equations were obtained (where  $t$  is in ns):

$$E(t)|_{\text{V/m}} = \begin{cases} -53330 \sin(0.1374275t), & 0 \leq t \leq 11.43 \text{ ns} \\ -53330 + 33822 \sin[0.0911664(t - 11.43)], & 11.43 < t \leq 28.66 \text{ ns} \\ -19684 + 19684 \sin[0.03915245(t - 28.66)], & 28.66 < t \leq 68.78 \text{ ns} \\ 7000 \sin[0.15707963(t - 68.78)], & 68.78 < t \leq 78.78 \text{ ns} \\ 7000 e^{-[0.150(t - 78.78)]}, & 78.78 < t \leq 114.78 \text{ ns.} \end{cases} \quad (5)$$

The time dependence prescribed by the above equations is sketched on an expanded time scale in Fig. 3(b). The time variations of currents calculated for the ankle, knee, heart,

and neck sections are given in parts (c) through (f) of Fig. 3. Peak induced currents calculated for the various sections of the body are compared in Table I with measured data [17]. For comparison the calculated values are scaled from 53.33

kV/m to 55.4 kV/m, which was typical of the values used for measurements. For the first set of comparisons, the agreement is fairly good.

For the EMP of Fig. 3(a) approximated by the time dependence shown in Fig. 3(b), we have calculated the total energy absorbed by the model to be 30.2 mJ. Shown in Table II are the specific absorptions (SA's) for the various organs as well as the whole body in mJ/kg for the EMP's of Fig. 3(b) and Fig. 5. The SA's are fairly small compared with whole-body-averaged values of the order of 28.88 J/kg per pulse that have been proposed for the 1990 revision of ANSI C95.1 Radiofrequency Protection Guide (RFPG) based on up to five pulses per 6 min.

Yet another, and perhaps the most convenient and accurate, procedure for these calculations was used for the measured EMP waveform sketched in Fig. 4. In this case the data were provided on a floppy disk, which made it very convenient to read it into the computer. The  $E$  field data as read into the computer are shown in Fig. 5. The time  $t = 0$  in Fig. 5 was started with the initial rise of the pulse. Since very low fields are involved beyond the first zero crossing and these result in relatively weak currents, the pulse was truncated at  $t = 356$  ns to save computation time.

The electric field values sketched in Fig. 4 as a function of time were available at 2 ns intervals on the floppy disk. For the FDTD method, the time step  $\delta t$  at which the data are needed is  $\delta/2c$  (where  $\delta$  is the cell size and  $c$  is the velocity of electromagnetic waves in air). For these calculations, we have used both the 5628 and the 45024 cell models of the human body, where cubical cells of dimensions 2.62 cm and 1.31 cm, respectively, are used to describe the volume-averaged tissue dielectric constants and conductivities for the various regions of the body. The values of  $\delta t$  needed for the two models are 0.04367 and 0.02183 ns, respectively. Since the provided data were available at 2 ns intervals, linear interpolation was used to obtain the incident  $E$  fields at these finer intervals of  $\delta t$ .

The time variations of currents for the ankle, knee, thigh (23.6 cms above the knee), heart, and neck sections are given in, respectively, parts (a) through (e) of Fig. 6. As previously observed from the measured data in Table I, albeit for a slightly different pulse shape (of Fig. 3), the highest peak currents are calculated for the section through the thighs. It is also interesting to note in parts (a)–(e) of Fig. 6 that there is little or no variation in the current profiles for the important initial peak current region between the 1.31 cm and 2.62 cm resolution models. This is especially surprising since some of these sections contain relatively few cells.

Since the time step,  $\delta t$ , required for the 1.31 cm model is exactly half that for the coarser 2.62 cm model and the number of cells involved is almost eight times greater (600704 versus 77064), the calculations with the 1.31 cm model are much more time intensive (by nearly a factor of 16) than those for the 2.62 cm model. The major purpose of using the 1.31 cm model, therefore, was to obtain the calculated distribution at the current peak with a higher resolution than that possible with the 2.62 cm model. The calculated current density contour diagrams are shown in parts (a) through (c) of Fig. 7 for the neck section and for sections of the body through the heart and the liver, respectively. These current densities have been calculated using the 1.31 cm model for times corresponding to the peak total current for the respective sections.

The total energy absorbed by the whole model for the EMP of Fig. 5 is calculated to be 15.4 mJ. Shown in Table II are the SA's calculated for the various organs for this EMP.

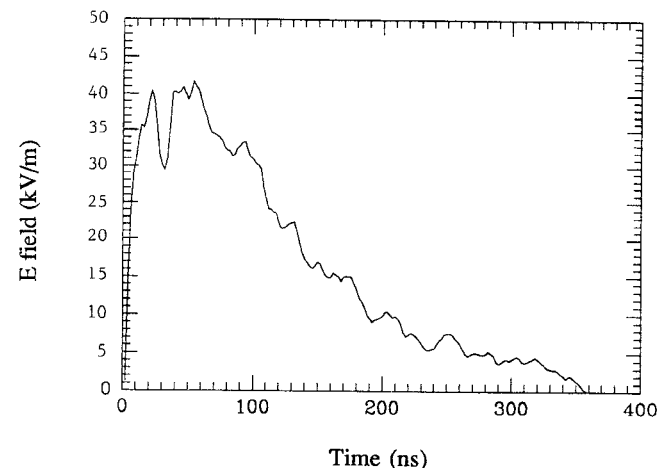


Fig. 5. The truncated EMP as read into the computer.

As mentioned earlier, these SA's are fairly small and considerably lower than the values proposed for the 1990 revision of ANSI C95.1 RFPG.

## V. CONCLUSIONS

The finite-difference time-domain method has been used to calculate coupling of an electromagnetic pulse to anatomically based models of the human body composed of cubical cells of dimensions 1.31 or 2.62 cm. The time variations of the induced currents are surprisingly similar for the 1.31 cm and 2.62 cm resolution models for the important initial region up to the current peak. Since the higher resolution model requires a much larger number of cells for the interaction space (almost 8:1) and a stepping time period that is half that for the coarser (2.62 cm cell size) model, it is very time intensive for the calculations. The main role of the finer model, therefore, is in calculating current distributions in the various parts of the body at the respective current peaks, i.e., up to the time corresponding to the current peak for the various sections. Since peak currents typically exist at times of the order of 11–12 ns after the onset of the pulse, the number of iterations needed for the higher resolution model is relatively small.<sup>1</sup>

Being a time-domain technique, the FDTD method is ideally suited for calculations involving EMP, allowing us to model the pulse shape exactly. Since the human body is dispersive, it would be desirable to modify the program so that time-domain descriptions of the tissue polarization can be incorporated to account for the relaxation mechanisms that are responsible for the frequency-dependent dielectric properties. Because the scope of the present effort did not call for a full-blown effort in this regard, we have used dielectric properties at 40 MHz in the first instance to get an estimate of the currents that are induced. This may, however, not be altogether erroneous since the predominant components of the induced currents are at frequencies close to 40–50 MHz because of the resonance of absorption of the adult, 1.75-m-tall human standing on a ground plane.

<sup>1</sup>A total of 700 iterations ( $\delta t = 0.02183$  ns) were used for the 1.31 cm resolution model. The computation time needed on the APOLLO workstation was approximately 420 min.

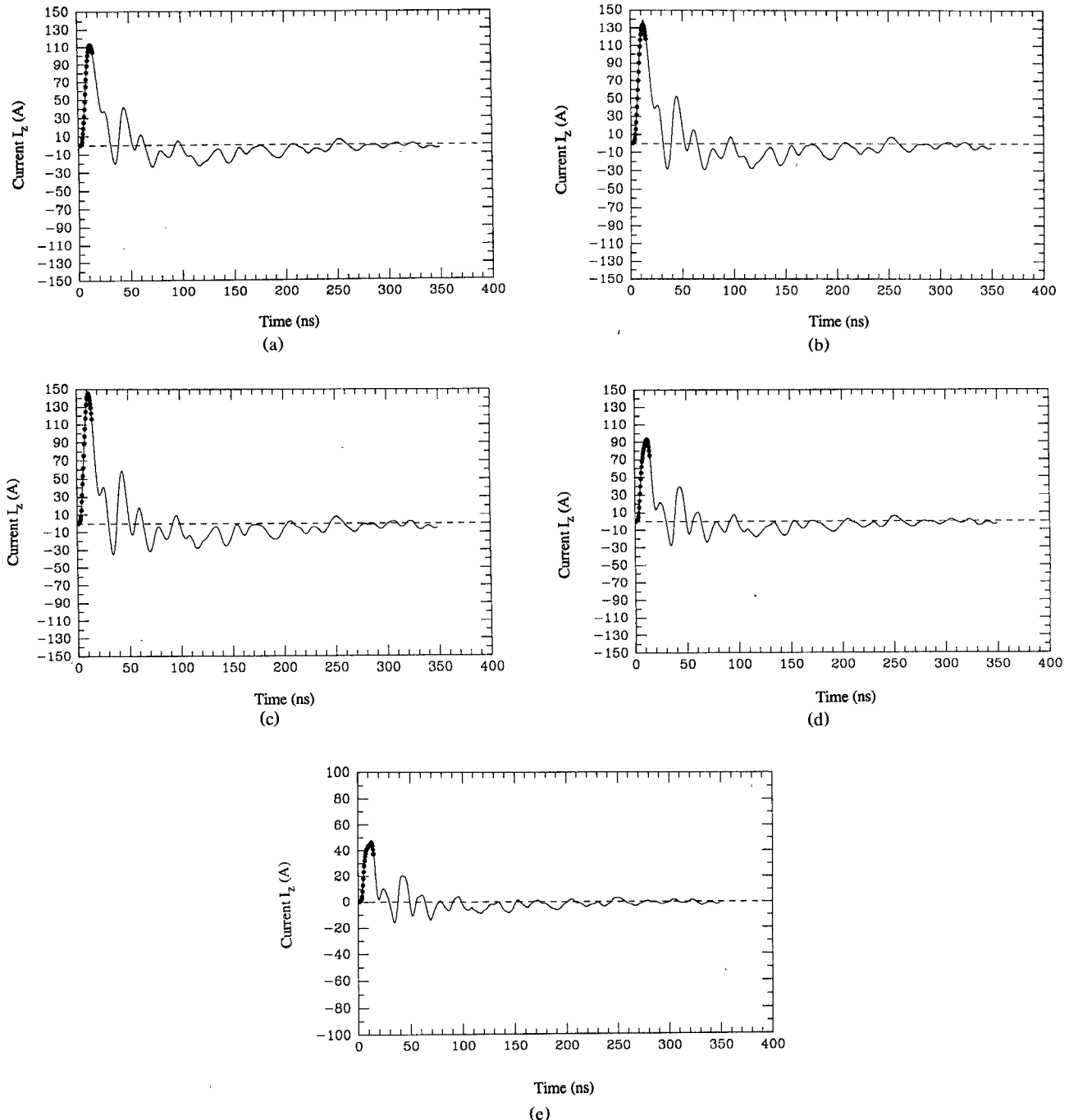


Fig. 6. Currents induced for the prescribed EMP of Fig. 5 using anatomically based models with cell sizes 2.62 cm (solid curve) and 1.31 cm (dots), respectively. Peak incident field = 41.5 kV/m. (a) Current for the section through the ankles. (b) Current for the section through the knees. (c) Current for the section through the thighs (23.6 cms above the knees). (d) Current for the section through the heart. (e) Current for the section through the neck.

The calculated currents for one of the EMP's are compared with data measured for a human subject for the various sections. The agreement for the first set of comparisons is fairly good. This is encouraging and lends support to the usefulness of an anatomically based model for obtaining induced current distributions as well as specific absorptions for the various organs.

It is interesting to note that there is very little energy absorbed by the human body because of the very limited time duration (50 ns or less) for which significant currents

can be induced. For the EMP's sketched in Figs. 3 and 4, we have calculated the total energy absorbed by the human body to be 30.2 and 15.4 mJ, respectively. The SA's for the various organs and the whole body are given in Table II. They are considerably smaller than the value of 28.8 J/kg whole-body-averaged SA per pulse that has been proposed for the 1990 revision of ANSI C95.1 RFPG. We are in no position to comment on the biological effects of high instantaneous currents of time durations 50 ns or less since very little is known about currents of such short duration.

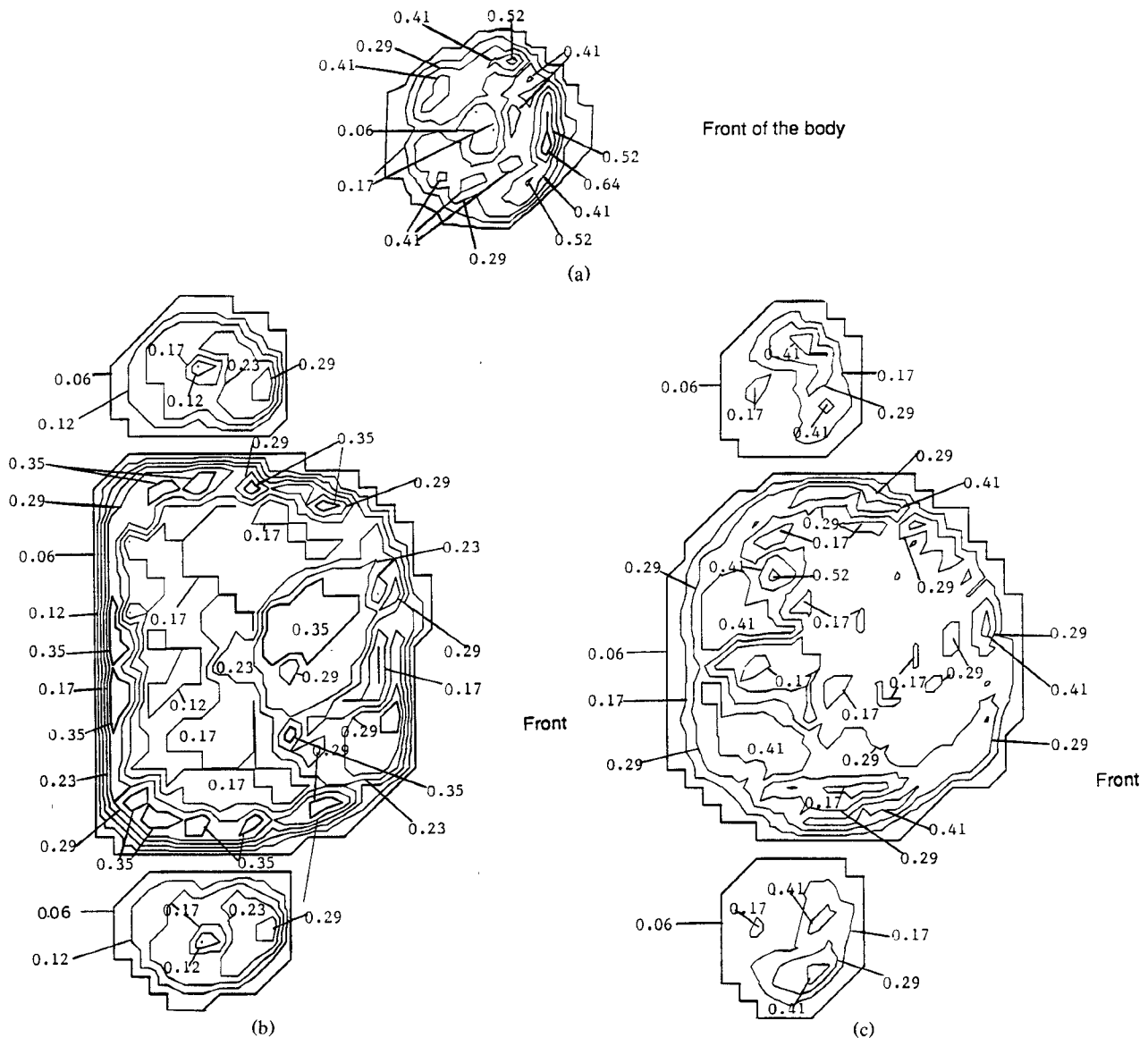


Fig. 7. Contours of constant current density ( $\text{A}/\text{cm}^2$ ) for the various sections of the anatomically based model with cell size = 1.31 cm. The time corresponding to the peak total current through the individual sections is taken. From Fig. 5, peak incident field = 41.5 kV/m. (a) The neck section (step size between contours =  $0.1165 \text{ A}/\text{cm}^2$ ). (b) The section through the heart (step size between contours =  $0.058 \text{ A}/\text{cm}^2$ ). (c) The section through the liver (step size between contours =  $0.1165 \text{ A}/\text{cm}^2$ ).

#### ACKNOWLEDGMENT

The authors have benefited from many useful discussions with Dr. D. Erwin and R. Bixby.

#### REFERENCES

- [1] K. L. Grønhaug, "Measurements of EMP induced currents in the human body," Report FFI/NOTAT-88/4038, Forsvarets Forsknings-institutt, Norwegian Defense Research Establishment, Box 25-N-2007, Kjeller, Norway, 1988.
- [2] A. W. Guy, "Analysis of time domain induced current and total absorbed energy in humans exposed to EMP electric fields," Final Report prepared for ERC Facilities Service Corp., 3211 Germantown Road, Fairfax, VA 22030, June 30, 1989.
- [3] G. J. Burke and A. J. Poggio, "Numerical electromagnetics code (NEC)—Method of moments," Lawrence Livermore National Laboratory, Livermore, CA.
- [4] D. M. Sullivan, O. P. Gandhi, and A. Taflove, "Use of the finite-difference time-domain method in calculating EM absorption in man models," *IEEE Trans. Biomed. Eng.*, vol. 35, pp. 179–186, 1988.
- [5] J. Y. Chen and O. P. Gandhi, "Electromagnetic deposition in an anatomically based model of man for leakage fields of a parallel-plate dielectric heater," *IEEE Trans. Microwave Theory Tech.*, vol. 37, pp. 174–180, 1989.
- [6] J. Y. Chen and O. P. Gandhi, "RF currents induced in an anatomically-based model of a human for plane-wave exposures (20–100 MHz)," *Health Phys.*, vol. 57, pp. 89–98, 1989.
- [7] K. S. Yee, "Numerical solution of initial boundary value problems involving Maxwell's equations of isotropic media," *IEEE Trans. Antennas Propagat.*, vol. AP-14, pp. 302–307, 1966.
- [8] K. Umashankar and A. Taflove, "A novel method to analyze electromagnetic scattering of complex objects," *IEEE Trans. Electromagn. Compat.*, vol. EMC-24, pp. 397–405, 1982.
- [9] R. Holland, "THREDE: A free-field EMP coupling and scattering code," *IEEE Trans. Nucl. Sci.*, vol. NS-24, pp. 2416–2421, 1977.

- [10] K. S. Kunz and K-M. Lee, "A three-dimensional finite-difference solution of the external response of an aircraft to a complex transient EM environment: Part 1—The method and its implementation," *IEEE Trans. Electromagn. Compat.*, vol. EMC-20, pp. 328–332, 1978.
- [11] A. Eycleshymer and D. M. Schoemaker, *A Cross-Section Anatomy*. New York: D. Appleton, 1911.
- [12] O. P. Gandhi, "State of the knowledge for electromagnetic absorbed dose in man and animals," *Proc. IEEE*, vol. 68, pp. 24–32, 1980.
- [13] D. M. Sullivan, D. T. Borup, and O. P. Gandhi, "Use of the finite-difference time-domain method in calculating absorption in human tissues," *IEEE Trans. Biomed. Eng.*, vol. BME-34, pp. 148–157, 1987.
- [14] C. Q. Wang and O. P. Gandhi, "Numerical simulation of annular phased arrays for anatomically based models using the FDTD method," *IEEE Trans. Microwave Theory Tech.*, vol. MTT-37, pp. 118–126, 1989.
- [15] C. C. Johnson and A. W. Guy, "Nonionizing electromagnetic wave effects in biological materials and systems," *Proc. IEEE*, vol. 60, pp. 692–718, 1972.
- [16] J. R. Mautz, "Mie series solution for a sphere," *IEEE Trans. Microwave Theory Tech.*, vol. MTT-26, p. 375, 1978.
- [17] W. Hammer *et al.*, personal communication.

✉



**Jin-Yuan Chen** (S'88–M'88) was born in Jiangsu, China, in 1945. He received the B.S. and M.S. degrees in electrical engineering from the University of Science and Technology of China (USTC) and Ph.D. degree, also in electrical engineering, from the University of Utah, Salt Lake City.

From 1970 to 1978 and from 1981 to 1983 he taught in the Department of Electrical Engineering at USTC. At the same time, he studied the frequency synthesizer, the measurement of high-stability and high-accuracy frequency sources, the

phase-locked millimeter-wave transmitter, the tracking and phase-locked millimeter-wave Doppler receiver, and the new millimeter-wave Gunn oscillator phase-locking method. Since 1983 he has been a research assistant and a research associate at the University of Utah. Currently research focuses on electromagnetic dosimetry and the numerical modeling of humans for exposures to far and near electromagnetic fields and electromagnetic pulses.

Dr. Chen was awarded the Guo Mou-ruo prize and a science research prize by the Chinese Academy of Sciences in 1981, 1982, and 1983 for his research. He received the best student scientific paper award at the 10th Annual Meeting of the Bioelectromagnetics Society, Stamford, CT, in 1988.

✉



**Om P. Gandhi** (S-57–M'58–SM'65–F'79) is a Professor of Electrical Engineering at the University of Utah, Salt Lake City. He is the author or coauthor of several book chapters, over 200 journal articles on microwave tubes, solid-state devices, and electromagnetic dosimetry, and the textbook *Microwave Engineering and Applications* (New York: Pergamon). He also recently edited the book *Biological Effects and Medical Applications of Electromagnetic Energy* (Prentice-Hall, 1990) and coedited the book *Electromagnetic Biointeraction* (Plenum Press, 1989).

Dr. Gandhi received the Distinguished Research Award from the University of Utah for 1979–1980 and a special award for "Outstanding Technical Achievement" from the IEEE, Utah Section, in 1975. He is Cochairman of the IEEE SCC 28.IV Subcommittee on RF Safety Standards and a past Chairman of the IEEE Committee on Man and Radiation (COMAR). His name is listed in *Who's Who in the World*, *Who's Who in America*, *Who's Who in Engineering*, and *Who's Who in Technology Today*.